https://doi.org/10.15407/scine21.06.038

JAVORSKYJ, I. M. [1] (https://orcid.org/0000-0003-0243-6652),
TORBA, Yu. I. [2] (https://orcid.org/0000-0001-8470-9049),
YUZEFOVYCH, R. M. [1, 3] (https://orcid.org/0000-0001-5546-453X),
SBRODOV, Ye. V. [2, 4] (https://orcid.org/0009-0005-7614-008X),
and LYCHAK, O. V. [1] (https://orcid.org/0000-0001-5559-1969)

[1] Karpenko Physico-Mechanical Institute
National Academy of Sciences of Ukraine,
5, Naukova St., Lviv, 79060, Ukraine,
+380 32 263 3088, pminasu@ipm.lviv.ua
[2] Joint Stock Company Zaporizhzhia Machine-Building Design
Bureau PROGRESS named after Academician O. H. Ivchenko,
2, Ivanova St., Zaporizhzhia, 69068, Ukraine,
+380 61 769 93 97, progress@ivchenko-progress.com
[3] Lviv Polytechnic National University,
12, Bandera St., Lviv, 79000, Ukraine,
+380 32 258 25 37, coffice@lpnu.ua
[4] National University "Zaporizhzhia Polytechnic,"
64, Zhukovskoho St., Zaporizhzhia, 69063, Ukraine,
+380 61 764 25 06, rector@zp.edu.ua

PERIODICALLY NON-STATIONARY PROPERTIES OF VIBRATIONS IN A GAS TURBINE ENGINE WITH AN UNBALANCED ROTOR

Introduction. *transform of the vibration signal, while the power spectrum has been estimated through the Blackman—Tukey method. However, because experimental vibration data are characterized by a combination of harmonic and stochastic processes, both techniques have proven inadequate for analyzing mixed signals.*

Problem Statement. *The evaluation of rotor balance in gas turbine engines has been commonly based on the magnitude of the regular co The amplitude spectrum of a gas turbine engine has traditionally been determined using the Fourier mponent of vibrations at the rotor's rotational frequency. Yet, the vibration signal contains numerous additional components, including stochastic ones, which should be accounted for to obtain reliable estimates. Modeling the vibration signal as a periodically non-stationary random process (PNRP) has allowed separating the deterministic and the stochastic components.*

Citation: Javorskyj, I. M., Torba, Yu. I., Yuzefovych, R. M., Sbrodov, Ye. V., and Lychak, O. V. (2025). Periodically Non-Stationary Properties of Vibrations in a Gas Turbine Engine with an Unbalanced Rotor. *Sci. innov.*, 21(6), 38—48. https://doi.org/10.15407/scine21.06.038

Purpose. *The study has aimed to conduct a comparative analysis of periodic non-stationarity in vibration signals of gas turbine engines with balanced and unbalanced rotors.*

Materials and Methods. *Vertical vibration components of balanced and unbalanced gas turbine engines in the low-frequency range (<2 kHz) have been analyzed. The vibration signal has been modeled as a periodically non-stationary random process, and an LS-functional has been applied to identify the fundamental frequencies of both deterministic and stochastic components.*

Results. *Correlation and spectral functions of vibration signals have been estimated, and the fundamental frequencies of their regular and stochastic components have been determined. It has been shown that the vibration spectra of engines with both balanced and unbalanced rotors are mixed. The deterministic component has exhibited a polyharmonic spectrum, and the harmonic amplitudes have been quantified. Furthermore, engine vibrations have been shown to exhibit second-order periodic non-stationarity.*

Conclusions. *The proposed vibration indicators have provided a basis for improving engine balancing during adjustment and repair procedures. The study has also highlighted the potential of these indicators for early detection of rotor defects. Future research will focus on analyzing the polyharmonic structure of vibration spectra and developing a refined methodology for defect diagnostics at incipient stages.*

Keywords: gas turbine engine, vibration, periodic non-stationary random processes, frequency estimation, average, variance.

It has been well established in the literature [1—14] that the vibrations of gas turbine engines with unbalanced rotors are characterized by peak values in their amplitude or power spectra at the frequency corresponding to the first harmonic of rotor rotation. The amplitude spectrum is typically obtained using the Fourier transform (FT) of the raw signal, while the power spectrum is commonly derived through the periodogram or the Blackman—Tukey spectral estimator. Numerous techniques have been developed to represent vibration signals in different ways [15—22].

When FT is applied, vibration time series are treated as segments of deterministic oscillations, whereas in power spectrum estimation they are regarded as realizations of stationary random processes. If experimental data are better represented as the sum of harmonic and random components, both approaches become inadequate, often leading to inconsistent results. Specifically, the amplitudes and power values of the harmonics can be estimated with significant errors.

In such cases, the identification of harmonics and the estimation of their amplitudes should be based on a vibration signal model formulated as a periodically non-stationary random process (PNRP). This modeling framework has been adopted in the present study.

AMPLITUDE AND POWER SPECTRUM OF THE RAW SIGNAL

Suppose that the analyzed signal $\xi(t)$ is the sum of stationary random process $\eta(t)$ and almost periodical function

$$s(t)=\sum_{k=-M}^{M} c_k e^{i\omega_k t},$$

where M is number of harmonics, ω_k and c_k are their frequencies and amplitudes. The signal sample values $\xi(nh)$ are acquired for $n\in[-K,K]$, $2K=\frac{\Theta}{h}$, Θ is the realization length, h is sampling interval. Then for the signal discrete time FT [23, 24] we have:

$$\hat{c}_\xi(\omega)=\frac{h}{2\pi}\sum_{n=-K}^{K}\left[\eta(nh)+s(nh)\right]e^{-i\omega_k nh}. \quad (1)$$

The mathematical expectation of (1) is equal to:

$$E\hat{c}_\xi(\omega)=\frac{h}{2\pi}\left[m_\eta\sum_{n=-K}^{K}e^{-i\omega_k nh}+\sum_{k=-M}^{M}c_k\sum_{n=-K}^{K}e^{-i(\omega-\omega_k)nh}\right],$$

where $m_\eta=E\eta(nh)$ is a mean of $\eta(nh)$. Assuming that $h\le\frac{\pi}{\omega_M}$ and using the formula for the sum of geometric progression we obtain

$$\sum_{n=-K}^{K}e^{-i\omega nh}=1+\sum_{n=1}^{K}\left(e^{i\omega nh}+e^{-i\omega nh}\right)=\varphi(\omega,K),$$

where

$$\varphi(\omega,K)=\frac{\sin\omega\left(K+\frac{1}{2}\right)h}{\sin\omega\frac{n}{2}}.$$

Hence

$$E\hat{c}_\xi(\omega)\approx\frac{h}{2\pi}\left[m_\eta\varphi(\omega,K)+\sum_{k=-M}^{M}c_k\varphi(\omega-\omega_k,K)\right].$$

Since $\varphi(0,K)=2K+1$ then for the large K we get:

$$E\hat{c}_\xi(\omega)\approx\frac{\Theta}{\pi}c_k. \quad (2)$$

It means that we cannot determine the amplitudes of harmonics for signal $\xi(t)=\eta(t)+s(t)$ using FT, because the values (2) are different according to realization length θ and $E\hat{c}(\omega_k)\to\infty$, as $\theta\to\infty$. Herewith the spectral properties of the random process in general do not characterize. These properties can be described using the higher moment functions of the random process.

The first well-known results in this field were obtained by the N. Wiener and A. Khinchin [23, 25]. They introduced concept of the power spectral density as the FT of the covariance function $R_\xi(u)=E\,\xi(t)\xi(t+u)$, $\xi(t)=\xi(t)-m_\xi(t)$:

$$f_\xi(\omega)=\frac{1}{2\pi}\int_{-\infty}^{\infty}R_\xi(u)e^{-i\omega u}du. \quad (3)$$

To estimate the power spectral density on the basis of experimental data the correlogram method of Blackman-Tukey can be used:

$$\hat{f}_\xi(\omega)=\frac{1}{2\pi}\int_{-u_m}^{u_m}\hat{R}_\xi(u)k(u)e^{-i\omega u}du,$$

here $\hat{R}_\xi(u)$ is the estimator of covariance function:

$$\hat{R}_\xi(u)=\frac{1}{K}\sum_{n=1}^{K}\left[\xi(nh)-\hat{m}\right]\cdot\left[\xi(nh+u)-\hat{m}\right],$$

$$\hat{m}=\frac{1}{K}\sum_{n=1}^{K}\xi(nh), \quad (4)$$

where $k(u)$ is the covariance window, u_m is cut-of point of the correlogram.

The discrete estimator of (3) has the form:

$$\hat{f}_\xi(\omega)=\frac{h}{2\pi}\sum_{n=-L}^{L}\hat{R}_\xi(nh)k(nh)e^{-i\omega nh}, \quad (5)$$

where $L=\frac{u_m}{h}$. For the asymptotic value of the mathematical expectation of (5) we find:

$$E\hat{f}_\xi(\omega)=\frac{h}{2\pi}\sum_{n=-L}^{L}R_\xi(nh)k(nh)e^{-i\omega nh}.$$

The time-averaged covariance function of the signal (its covariance function in the stationary approximation) is equal to:

$$\hat{R}_\xi(nh)=\hat{R}_\eta(nh)+\sum_{k=-M}^{M}|c_k|^2e^{i\omega_k nh}. \quad (6)$$

Assume for simplicity that the covariance window is rectangular:

$$k(u)=\begin{cases}1, |u|\le u_m,\\ 0, |u|>u_m.\end{cases}$$

Then [25]

$$E\hat{f}_\xi(\omega)=\int_{-\infty}^{\infty}f_\eta(\omega_1)\lambda(\omega-\omega_1)d\omega_1+$$

$$+\frac{h}{2\pi}\sum_{k=-M}^{M}|c_k|^2\varphi(\omega-\omega_k,L).$$

Since $\varphi(0,L)=2L+1$, then the peak values $E\hat{f}_\xi(\omega)$ are proportional to u_m. Therefore searching for these peaks we can only find the frequencie.

ANALYSIS OF THE SPECTRAL COMPOSITION OF GAS-TURBINE ENGINE VIBRATION

We shall analyze the vertical component of low-frequency vibration (<2 kHz), which were acquired from gas-turbine engine without failure and engine with unbalanced rotor. The covariance function estimators for these different cases, which were calculated using formulae (4) are shown in Fig. 1. In Fig. 2 the respective estimators of the power spectral densities are presented, herewith Hamming window was used.

As we can see, both covariance functions contain the random components with rapidly and slowly damping correlations as well as undamped oscillations. The total signal power in the second case (13.63 g^2) is essentially larger than in the first (3.83 g^2). The availability of the undamped oscilla-

tions, as it follows from equation (6), can testify about the presence in the signal composition of the deterministic harmonic components, herewith the total power of these components is much higher in the case of engine with the unbalanced rotor. This results in the mixed power spectra of the signals. It means that the peak values in Fig. 2 can be caused both by the powers of deterministic harmonics and the values of narrow-band spectral densities of the random components. To divide the deterministic and random components we use the method for discovering of the first order hidden periodicities [25].

HARMONIC ANALYSIS OF THE DETERMINISTIC OSCILLATIONS

The estimation of the basic frequencies of the deterministic components is the first issue of the vibration harmonic analysis. To find the basic frequencies, the special functionals can be used [25—27], that are similar to the PNRP coherent or component statistics for mean function estimators with the except that test basic frequency is inserted to replace the true period. These functionals have extreme values at the points, which are asymptotically unbiased and consistent basic frequency estimators. To improve the efficiency of estimating of basic frequencies, the least square (LS) method was proposed in [28]. As the signal realization length increases, the LS functional for determining of the basic frequencies of the mean function quickly tends to

$$\hat{F}_1(f)=\frac{1}{2}\sum_{k=1}^{L_i}\left[\left[\hat{m}_k^c(f)\right]^2+\left[\hat{m}_k^s(f)\right]^2\right], \qquad (7)$$

where

$$\begin{Bmatrix}\hat{m}_k^c(f)\\ \hat{m}_k^s(f)\end{Bmatrix}=\frac{2}{2K+1}\sum_{n=-K}^{K}\xi(nh)\begin{Bmatrix}\cos(2k\pi fnh)\\ \sin(2k\pi fnh)\end{Bmatrix},$$

and 2Θ is the realization length, $h = \Theta/K$ is the sampling step and L_i is number of harmonics for each component, f is a test frequency. The maximum points $\hat{f}_0^{(i)}$ of (7) is asymptotically unbiased and consistent estimator for the mean basic frequency. The functional (7) at the maximum point $f=\hat{f}_0^{(i)}$ is close to the sum of time-averaged power of the chosen harmonics:

$$\hat{F}_1\left(\hat{f}_0^{(i)}\right)=\hat{P}_t^{(d_i)}=\frac{1}{2}\sum_{k=1}^{L_i}\left[\left[\hat{m}_k^c\left(\hat{f}_0^{(i)}\right)\right]^2+\left[\hat{m}_k^s\left(\hat{f}_0^{(i)}\right)\right]^2\right].$$

The quantities $\hat{m}_k^c\left(\hat{f}_0^{(i)}\right)$ and $\hat{m}_k^s\left(\hat{f}_0^{(i)}\right)$ are asymptotically unbiased and consistent estimators of the Fourier coefficients for the mean function of each component. Hence, we can form the mean function estimator for each component:

$$\hat{m}_i(t)=\sum_{k=1}^{L_i}\left[\hat{m}_k^c\left(\hat{f}_0^{(i)}\right)\cos 2k\pi\hat{f}_0^{(i)}t+\right.$$
$$\left.+\hat{m}_k^s\left(\hat{f}_0^{(i)}\right)\sin 2k\pi\hat{f}_0^{(i)}t\right]. \qquad (8)$$

The functions (8) describe the deterministic components of vibrations.

We calculated the functional (7) changing the test frequency f in the neighborhood of the points at which the spectral density estimator reaches its maximum values (Fig. 2). The deterministic harmonics, whose frequencies are close to the maximum points of the spectral density, were displayed over all low-frequency interval. The graphs of the dependencies for $\hat{F}_1(f)$ on test frequency in different intervals for healthy (balanced) and faulty (unbalanced) engines are shown in Fig. 3. The first dependence was calculated for $L_1 = 9$, the second — for $L_1 = 3$. The peak values of $\hat{F}_1(f)$ in both cases are clearly visible, and the maximum points $\hat{f}_0^{(i)}$ are

Table 1. **Maximum Points and Amplitudes of the First Harmonics**

Balanced engine		Unbalanced engine	
$\hat{f}_0^{(i)}$, Hz	$A\left(\hat{f}_0^{(i)}\right)$, g	$\hat{f}_0^{(i)}$, Hz	$A\left(\hat{f}_0^{(i)}\right)$, g
49.98	0.56	49.98	1.14
533.37	0.67	533.62	3.59
720.94	0.46	714.99	0.92
721.80	0.59	715.76	0.98
1129.72	0.48	716.45	1.61

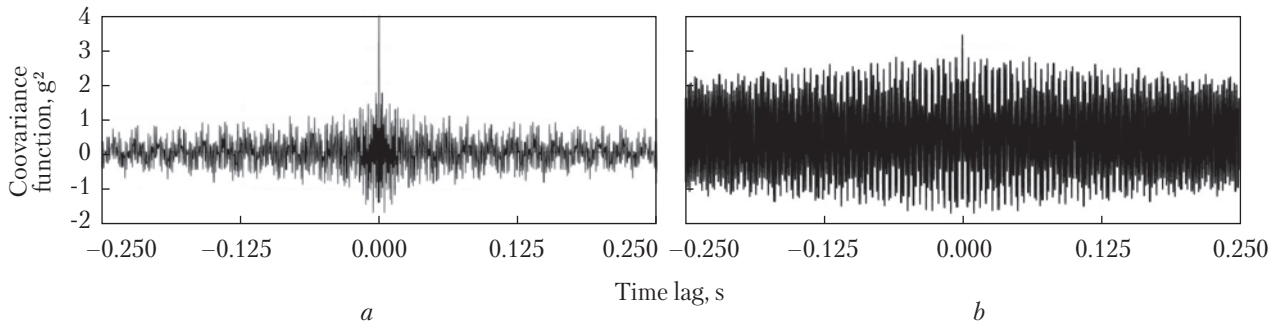

Fig. 1. Estimators of the covariance function of the balanced (*a*) and unbalanced (*b*) engines

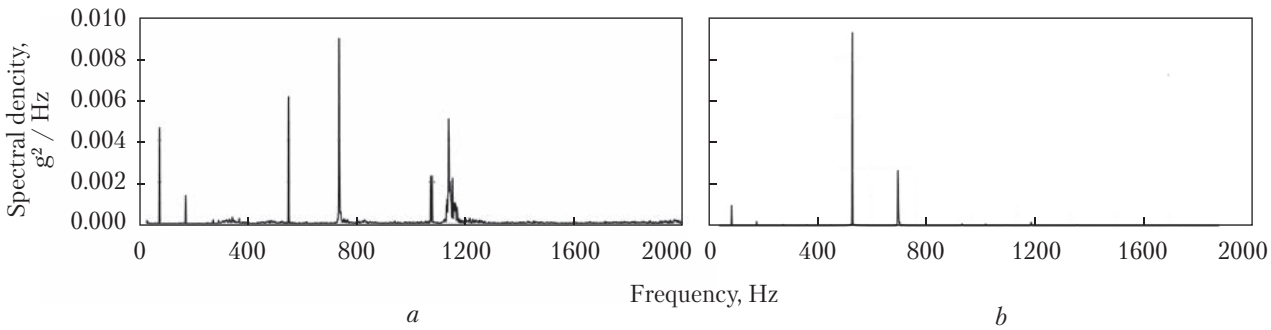

Fig. 2. Estimators of the power spectral densities for the balanced (*a*) and unbalanced (*b*) engines

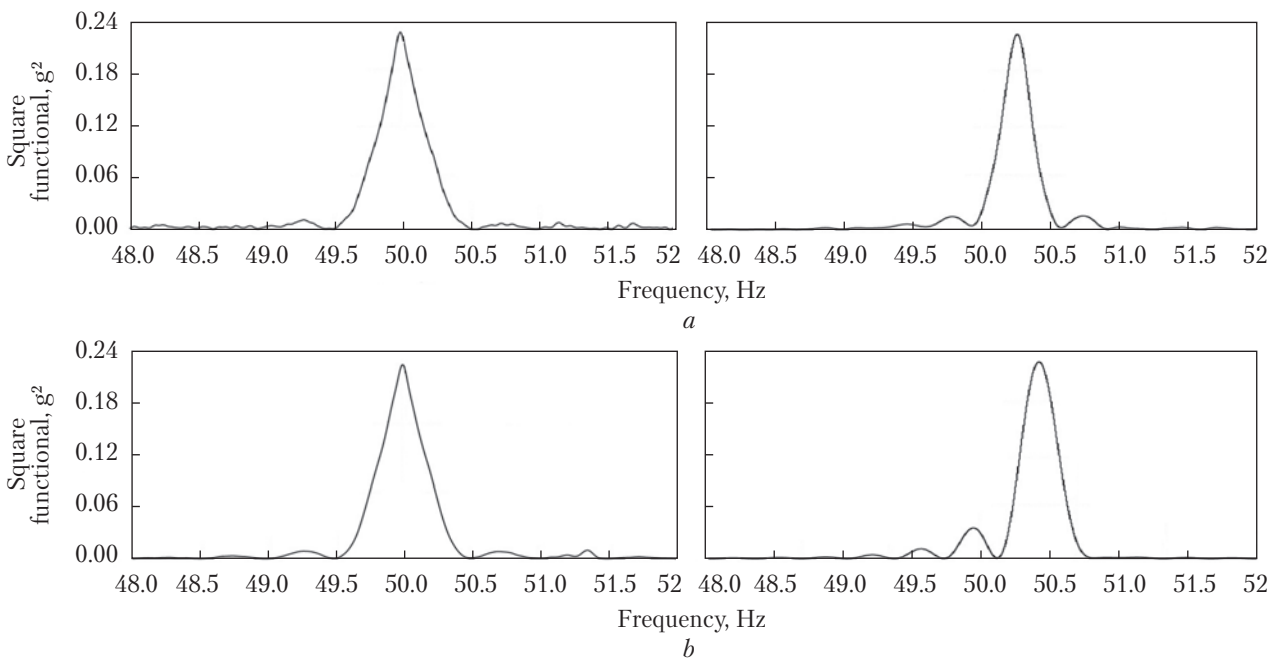

Fig. 3. Dependences of functional $F_1(f)$ on test frequency for balanced (*a*) and unbalanced (*b*) engines in different interval

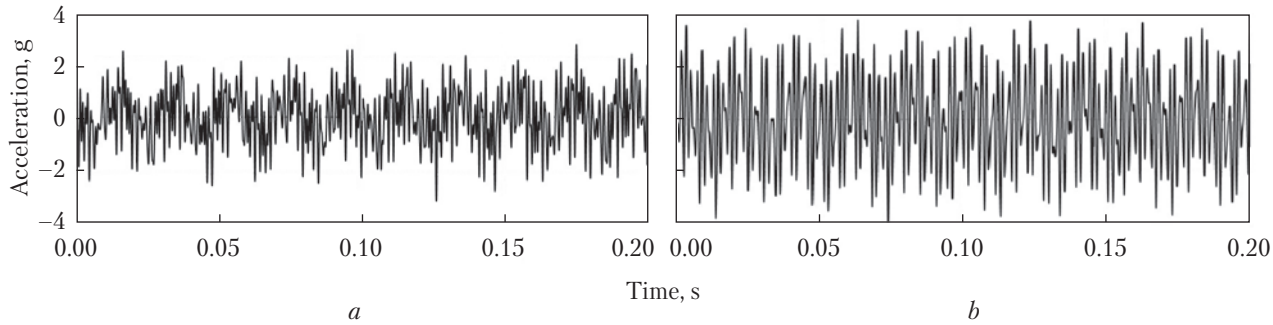

Fig. 4. Deterministic components of vibration for balanced (*a*) and unbalanced (*b*) engines

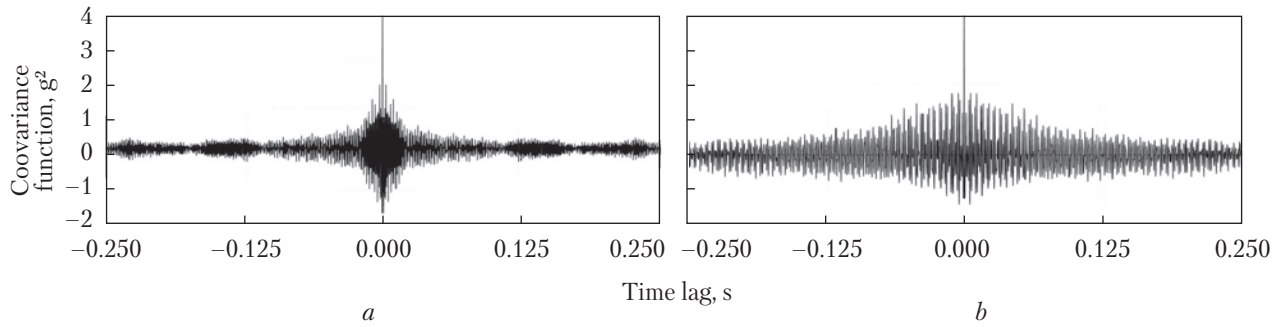

Fig. 5. Covariance function for balanced (*a*) and unbalanced (*b*) engines

easily determined. The obtained above also relate to another peaks of $\hat{F}_1(f)$, which are revealed for $L_3 = L_4 = 3$, $L_5 = 1$. Knowing $\hat{f}_0^{(i)}$ we calculate the amplitudes of the respective harmonics $A\left(k\hat{f}_0^{(i)}\right) = \left[\left[m_k^c\left(\hat{f}_0^{(i)}\right)\right]^2 + \left[m_k^s\left(\hat{f}_0^{(i)}\right)\right]^2\right]^{\frac{1}{2}}$. The maximum point of the functional $\hat{f}_0^{(i)}$ and its values $F_1\left(\hat{f}_0^{(i)}\right)$ for the balanced and unbalanced engines are given in Table 1. As we can see, the amplitude spectrum of deterministic oscillations contains except the harmonics with the frequency of the supply current 49.98 Hz and the rotor rotation frequency 539.62 Hz, also the harmonics with higher frequencies. The amplitudes of all harmonics for the balanced engine are small and their values differ insignificantly. The values of all amplitudes increases as the fault occurs, however the amplitude of harmonic with rotation frequency increases most of all. The ratio of the amplitudes for the different engine state is equal to: $\dfrac{A^{(f)}\left(k\hat{f}_0^{(2)}\right)}{A^{(h)}\left(k\hat{f}_0^{(2)}\right)} = 5.36.$

The harmonic power in the second case becomes more then twenty-eight times as much as in the first case. Then we can choose the ratio $I_1 = \dfrac{\left[A^{(f)}\left(k\hat{f}_0^{(2)}\right)\right]^2}{\left[A^{(h)}\left(k\hat{f}_0^{(2)}\right)\right]^2}$ as one of the indicators for the description of the rotor state.

Using the interpolation formula (8) we obtain the time dependence of each component $\hat{m}_i(t)$ of the deterministic oscillations. Their sum $\hat{m}(t) = \sum_{k=1}^{5}\hat{m}_k(t)$ is presented in Fig. 4 for the balanced and unbalanced engines. We can see, that oscillation power for the engine with unbalanced rotor is much more, herewith the oscillations with rotating frequency are distinguishable.

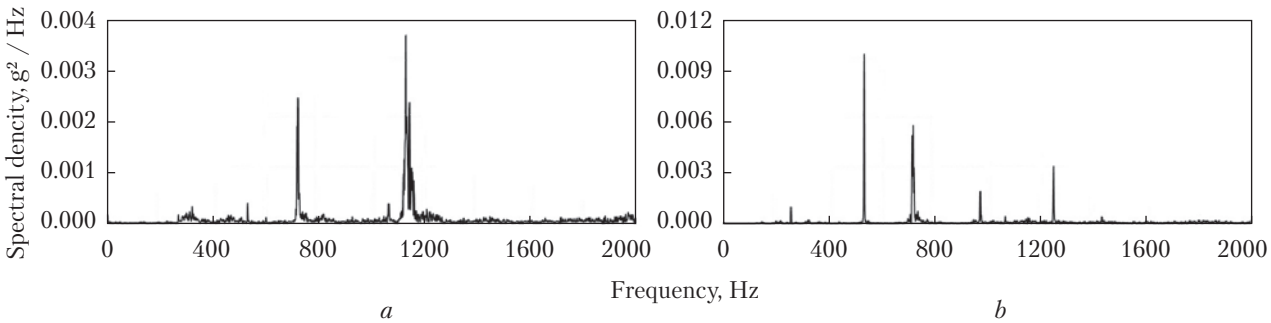

Fig. 6. Power spectral density for balanced (*a*) and unbalanced (*b*) engines

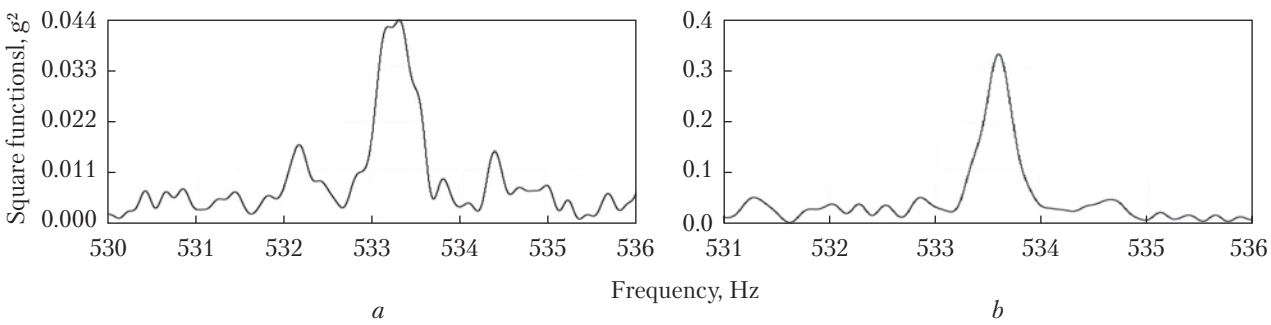

Fig. 7. Dependence of functional $F_2(f)$ on test frequency for balanced (*a*) and unbalanced (*b*) engines

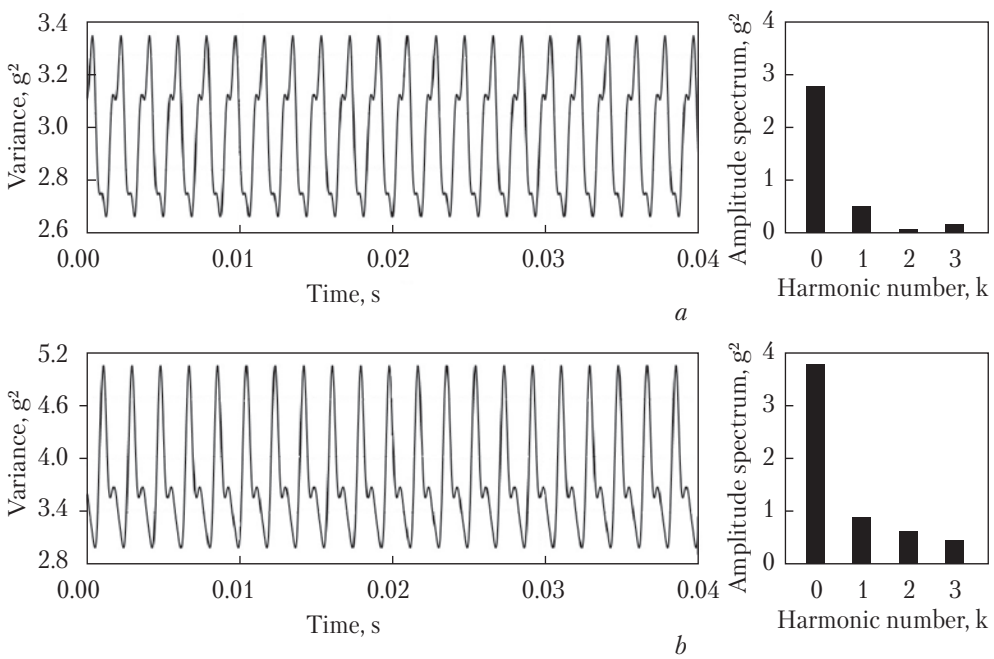

Fig. 8. Variance time dependences and their amplitude spectra for balanced (*a*) and unbalanced (*b*) engines

ISSN 2409-9066. Sci. innov. 2025. 21(6)

ANALYSIS OF STOCHASTIC OSCILLATIONS

Removing the deterministic oscillations $\hat{m}(t)$ from the realization of the raw vibration signal $\xi(nh)$ we obtain the stochastic part of vibration $\overset{\circ}{\xi}(nh) = \xi(nh) - \hat{m}(nh)$. The estimators of the power spectral density for the stochastic oscillations, which are calculated for the healthy and faulty engines, were shown in Fig. 5. It can be seen, that the power spectral density estimators contain both wide-band and narrow-band components. This is also observed on the graphs for the covariance function estimators. They quickly damp for the initial lags and have the form of the damped oscillations for further lags (Fig. 6). The total power of the stochastic oscillations for the healthy engine is 2.95 g^2, for the faulty one is 3.75 g^2. While the power of deterministic oscillations is respecting equal to 0.88 g^2 and 9.89 g^2.

To reveal the periodicity of time changes of the vibration variance we use the functional [28]:

$$\hat{F}_2(f) = \frac{1}{2}\sum_{k=1}^{L_2}\left[\left[\hat{R}_k^c(0,f)\right]^2 + \left[\hat{R}_k^s(0,f)\right]^2\right], \quad (9)$$

where

$$\begin{Bmatrix}\hat{R}_k^c(0,f)\\ \hat{R}_k^s(0,f)\end{Bmatrix} = \frac{2}{2K+1}\sum_{n=-K}^{K}\overset{\circ}{\xi}(nh)\begin{Bmatrix}\cos 2k\pi fnh\\ \sin 2k\pi fnh\end{Bmatrix}, \quad (10)$$

and L_2 is the number of its harmonics. The maximum points of expression (9) is an asymptotically unbiased and consistent estimator for the variation basic frequency. By substituting $f = \hat{f}_0$ into (10) we obtain statistics $\hat{R}_k^c(0,f)$ and $\hat{R}_k^s(0,f)$ for calculating Fourier coefficients of the variance. Hence, the quantities

$$\hat{F}_2\left(\hat{f}_0\right) = \frac{1}{2}\sum_{k=1}^{L_2}\left[\left[R_k^c\left(0,\hat{f}_0\right)\right]^2 + \left[R_k^s\left(0,\hat{f}_0\right)\right]^2\right]$$

defines the time-averaged power of time changes of variance.

Using the interpolation formula

$$\hat{R}\left(0,t,\hat{f}_0\right) = \hat{R}_0(0) + \sum_{k=1}^{L_2}\left[\hat{R}_k^c\left(0,\hat{f}_0\right)\cos 2k\pi\hat{f}_0 t + \hat{R}_k^s\left(0,\hat{f}_0\right)\sin 2k\pi\hat{f}_0 t\right]. \quad (11)$$

where

$$\hat{R}_0(0) = \frac{1}{2K+1}\sum_{n=-K}^{K}\overset{\circ}{\xi}{}^2(nh),$$

we can determine the variance estimator for all $t \in \left[0, \hat{f}_0^{-1}\right]$.

To search for the time periodicity of the variance we take $L_2 = 3$ in the formula (9) and change the test frequency in interval [531 Hz, 536 Hz]. The results of calculation are presented for the healthy and faulty engines by graphs in Fig. 7, *a, b*.

The maximum values of the functional $\hat{F}_2(f)$ are observed both for healthy and faulty engines. However the peak for the latter is much sharper and its height, which is defined by the total power of the variance harmonics, is more than seven times as much as one for the healthy engine. The maximum values are respectively equal to $\hat{f}_0^{(h)} = 533.605$ Hz and $\hat{f}_0^{(f)} = 533.309$ Hz, i.e. they differ only by digits after decimal points. Taking the obtained values $\hat{f}_0^{(h)}$ and $\hat{f}_0^{(f)}$ as the basic frequencies and substituting them into the expressions (11) we can calculate the Fourier coefficients of the variances and amplitudes

$$\hat{V}\left(k\hat{f}_0^{(h,f)}\right) = \left[\left[R_k^c\left(0,\hat{f}_0^{(h,f)}\right)\right]^2 + \left[R_k^s\left(0,\hat{f}_0^{(h,f)}\right)\right]^2\right]^{\frac{1}{2}}.$$

The amplitudes are given in Table 2. The amplitude spectra for the variance time changes are shown in Fig. 8, *a, b*.

Summing the harmonic amplitudes, we can find the measure of non-stationarity of the second order $I = \sum_{k=1}^{3}\frac{\hat{V}\left(k\hat{f}_0^{(h,f)}\right)}{\hat{V}^{(h,f)}(0)}$. This measure is respectively equal to 0.14 and 0.34 healthy and faulty engines. The amplitudes of the basic harmonics are the largest in the both cases. The oscillations with the basic frequencies are also most of all visible on the graphs

Table 2. **Amplitudes of Variance Harmonic for Different States**

Status	$\hat{V}(0)$, g^2	$\hat{V}(f_0)$, g^2	$\hat{V}(2f_0)$, g^2	$\hat{V}(3f_0)$, g^2
Healthy	2.925	0.280	0.041	0.081
Faulty	3.755	0.661	0.456	0.143

for variance time dependencies, which were obtained using interpolation formula (10). The oscillation swing is less than one for the healthy engine, while the near two for the engine with unbalanced rotor. Herewith the time-averaged variance value increases by $\Delta\hat{V}(0)=\hat{V}^{(f)}(0)-\hat{V}^{(h)}(0)=0.83\ \mathrm{g}^2$. It is desirable to add this quantity to the expression for the second indicator for the engine state description. Then we have $I_2=\dfrac{\left[\Delta\hat{V}(0)+\sum_{k=1}^{3}\hat{V}_k^{(f)}(0)\right]}{V(0)}=$ $= 0.56$. The indicator I_2 and also the indicator I_1 can be used for the engine state monitoring.

CONCLUSIONS

It has been shown that the vibration spectra of gas turbine engines with both balanced and unbalanced rotors are mixed, containing deterministic and stochastic components. Using the PNRP approach, these components have been separated, allowing the identification and analysis of hidden first- and second-order periodicities. The amplitude spectra of the deterministic oscillations have been revealed to be polyharmonic, and the corresponding harmonic amplitudes have been determined. Engines with unbalanced rotors have demonstrated the greatest increase in power at the harmonic corresponding to the rotation frequency. Furthermore, the vibrations have exhibited properties of second-order periodic non-stationarity, with the degree of non-stationarity increasing in the unbalanced case. Finally, new diagnostic indicators have been proposed that account for variations in the powers of deterministic and stochastic components, as well as in the time-dependent changes of vibration variance.

REFERENCES

1. Djaidir, B., Hafaifa, A., Kouzou, A. (2017). Faults detection in gas turbine rotor using vibration analysis under varying conditions. *J. theoretical and applied mechanics,* 55(2), 393—406. https://doi.org/10.15632/jtam-pl.55.2.393
2. Fábry, S., Češkovič, M. (2017). Aircraft gas turbine engine vibration diagnostics. *Review Articles,* 5(4), 24—28. https://doi.org/10.14311/MAD.2017.04.04
3. Pérez-Ruiz, J. L., Luis, J., Tang, Yu., Loboda, I., Miró-Zárate, L. A. (2024). An Integrated Monitoring, Diagnostics, and Prognostics System for Aero-Engines under Long-Term Performance Deterioration. *Aerospace,* 11(3), 217. https://doi.org/10.3390/aerospace11030217.
4. Rath, N., Mishra, R., Kushari, A. (2022). Aero engine health monitoring, diagnostics and prognostics for condition-based maintenance: an overview. *Int. J. Turbo Jet. Engines.* 40(s1), s279—s292. https://doi.org/10.1515/tjeng-2022-0020
5. Grządziela, A. (2006). Analysis of vibration parameters of ship gas turbine engines. *Polish Maritime Research*, 13(2), 22—26. URL: https://journal.mostwiedzy.pl/pmr/article/view/1230/1156 (Last accessed: 07.07.2025).
6. Fentaye, A. D., Baheta, A. T., Gilani, S. I., Kyprianidis, K. G. (2019). A review on gas turbine gas-path diagnostics: state-of-the-art methods, challenges and opportunities. *Aerospace*, 6(7), 83. https://doi.org/10.3390/aerospace6070083
7. Mishra, R. K., Thomas, J., Srinivasan, K., Nandi, V., Bhatt, R. R. (2015). Investigation of HP turbine blade failure in a military turbofan engine. *Int. J. Turbo Jet Engines*, 34(1), 23—31. https://doi.org/10.1515/tjj-2015-0049
8. Hanachi, H., Mechefske, C., Liu, J., Banerjee, A., Chen, Y. (2018). Performance-based gas turbine health monitoring, diagnostics, and prognostics: a survey. *IEEE Trans. Reliab.*, 67(3), 1340—1363. https://doi.org/10.1109/tr.2018.2822702
9. Tahan, M., Tsoutsanis, E., Muhammad, M., Karim, A. (2017). Performance-based health monitoring, diagnostics and prognostics for condition-based maintenance of gas turbines: A review. *Appl. Energy*, 198, 122—144. https://doi.org/10.1016/j.apenergy.2017.04.048
10. Zaidan, M., Relan, R., Mills, A., Harrison, R. (2015). Prognostics of gas turbine engine: An integrated approach. *Expert Systems with Applications*, 42(22), 8472—8483. https://doi.org/10.1016/j.eswa.2015.07.003
11. Stamatis, A. G. (2011). Evaluation of gas path analysis methods for gas turbine diagnosis. *J. Mech. Sci. Technol.*, 25(2), 469—477. https://doi.org/10.1007/s12206-010-1207-5
12. Heng, A., Zhang, S., Tan, A., Mathew, J. (2009) Rotating machinery prognostics: state of the art, challenges and opportunities. *Mech. Syst. Signal Process.*, 23(3), 724—739. https://doi.org/10.1016/j.ymssp.2008.06.009

13. Muszynska, A. (1995). Vibrational Diagnostics of Rotating Machinery Malfunctions. *Int. J. Rotating Machinery*, 1(3—4), 237—266. https://doi.org/10.1155/S1023621X95000108
14. Jardine, A., Lin, D., Banjevic, D. (2006). A review on machinery diagnostics and prognostics implementing condition-based maintenance. *Mech. Syst. Signal Process.,* 20(7), 1483—1510. https://doi.org/10.1016/j.ymssp.2005.09.012
15. Jiang, X., Yang, S., Wang, F., Xu, S., Wang, X., Cheng, X. (2021). OrbitNet: A new CNN model for automatic fault diagnostics of turbomachines. *Applied Soft Computing*, 110, 107702. https://doi.org/10.1016/j.asoc.2021.107702
16. Wang, C., Chen, C. (2001). Bifurcation of Self-Acting Gas Journal Bearings. *ASME J. Tribol.,* 123(4), 755—767. https://doi.org/10.1115/1.1388302
17. Aretakis, N., Mathioudakis, K., Kefalakis, M., Papailiou, K. (2004). Turbocharger Unstable Operation Diagnosis Using Vibroacoustic Measurements. *ASME. J. Eng. Gas Turbines Power,* 126(4), 840—847. https://doi.org/10.1115/1.1771686
18. Bonello, P., Pham, H. M. (2014). Nonlinear Dynamic Analysis of High Speed Oil-Free Turbomachinery With Focus on Stability and Self-Excited Vibration. *ASME. J. Tribol.*, 136(4), 041705. https://doi.org/10.1115/1.4027859
19. Soleimani, M., Campean, F., Neagu, D. (2021). Diagnostics and prognostics for complex systems: a review of methods and challenges. *Qual. Reliab. Eng. Int.*, 37(7), 3746—3778. https://doi.org/10.1002/qre.2947
20. Lakshminarasimha, A. N., Boyce, M. P., Meher-Homji, C. B. (1994). Modeling and analysis of gas turbine performance deterioration. *J. Eng. Gas Turbines Power*, 116(1), 46—52. https://doi.org/10.1115/1.2906808
21. Marinai, L., Probert, D., Singh, R. (2004). Prospects for aero gas-turbine diagnostics: a review. *Appl. Energy*, 79(1), 109—126. https://doi.org/10.1016/j.apenergy.2003.10.005
22. Napolitano, A. (2020). *Cyclostationary processes and time series: Theory, applications, and generalizations.* Elsevier, Academic Press, 2020. https://doi.org/10.1016/C2017-0-04240-4
23. Koopmans, L. H. (1974). *The spectral analysis of time series [by] L. H. Koopmans*. New York.
24. Kay, S. M. (1988). *Modern Spectral Estimation: Theory and Application*. New Jersey.
25. Javorskyj, I. (2013). *Mathematical models and analysis of stochastic oscillations.* Lviv [in Ukrainian].
26. Javorskyj, I., Matsko, I., Yuzefovych, R., Lychak, O., Lys, R. (2021). Methods of hidden periodicity discovering for gearbox fault detection. *Sensors*, 21(18), 6138. https://doi.org/10.3390/s21186138
27. Javorskyj, I., Yuzefovych, R., Matsko, I., Zakrzewski, Z., Majewski, J. (2017). Coherent covariance analysis of periodically correlated random processes for unknown non-stationarity period. *Dig. Signal Process.*, 65, 27—51. https://doi.org/10.1016/j.dsp.2017.02.013
28. Javorskyj, I., Yuzefovych, R., Matsko, I., Zakrzewski, Z. (2022). The least square estimation of the basic frequency for periodically non-stationary random signals. *Dig. Sign. Proc.*, 122, 103333. https://doi.org/10.1016/j.dsp.2021.103333
29. Javorskyj, I., Yuzefovych, R., Lychak, O., Semenov, P., Sliepko, R. (2023). Detection of distributed and localized faults in rotating machines using periodically non-stationary covariance analysis of vibrations. *Measurement Science and Technology*, 34(6), 065102. https://doi.org/10.1088/1361-6501/acbc93

Received 24.09.2024
Revised 10.03.2025
Accepted 25.03.2025

І.М. Яворський [1] (https://orcid.org/0000-0003-0243-6652),
Ю.І. Торба [2] (https://orcid.org/0000-0001-8470-9049),
Р.М. Юзефович [1, 3] (https://orcid.org/0000-0001-5546-453X),
Є.В. Сбродов [2, 4] (https://orcid.org/0009-0005-7614-008X),
О.В. Личак [1] (https://orcid.org/0000-0001-5559-1969)

[1] Фізико-механічний інститут ім. Г.В. Карпенка
Національної академії наук України,
вул. Наукова, 5, Львів, 79060, Україна,
+380 32 263 3088, pminasu@ipm.lviv.ua
[2] Акціонерне товариство «Запорізьке машинобудівне
конструкторське бюро ПРОГРЕС імені академіка О.Г. Івченка»,
вул. Іванова, 2, Запоріжжя, 69068, Україна,
+380 61 769 93 97, progress@ivchenko-progress.com
[3] Національний університет «Львівська політехніка»,
вул. Степана Бандери, 12, Львів, 79000, Україна,
+380 32 258 25 37, coffice@lpnu.ua
[4] Національний університет «Запорізька політехніка»,
вул. Жуковського, 64, Запоріжжя, 69063, Україна,
+380 61 764 25 06, rector@zp.edu.ua

ПЕРІОДИЧНО-НЕСТАЦІОНАРНІ ВЛАСТИВОСТІ ВІБРАЦІЙ ГАЗОТУРБІННОГО ДВИГУНА З НЕБАЛАНСОВАНИМ РОТОРОМ

Вступ. Амплітудний спектр вібрацій газотурбінного двигуна визначається за допомогою перетворення Фур'є сигналу, а спектр потужності — спектрального перетворення Блекмана-Тьюкі. Оскільки експериментальні дані описуються сумою гармонічного і випадкового процесів, то обидві процедури є неадекватними при аналізі мішаних сигналів.

Проблематика. Аналіз стану балансування роторів газотурбінних двигунів проводять на основі величини регулярної складової вібрацій на частоті обертання ротора. У складі вібраційного сигналу присутні низка різних, зокрема й стохастичних, компонент, які слід врахувати при обробці сигналу для отримання його реальних оцінок. Використання моделі вібраційного сигналу як періодично нестаціонарного випадкового процесу (ПНВП) дозволяє коректно розділити регулярну/детерміновану та стохастичну складові.

Мета. Порівняльний аналіз періодичної нестаціонарності вібраційних сигналів газотурбінних двигунів з небалансованим і добалансованим роторами.

Матеріали й методи. Аналіз вертикальних складових вібраційних сигналів небалансованого та добалансованого газотурбінних двигунів проведено у низькочастотній області (<2 кГц). Застосовано модель вібраційного сигналу газотурбінного двигуна як періодично нестаціонарного випадкового процесу та МНК-функціонал для визначення базових частот детермінованих та стохастичних складових сигналу.

Результати. Оцінено кореляційні та спектральні функції вібраційних сигналів, базові частоти їхніх регулярних та стохастичних складових. Показано, що спектри вібрацій газотурбінного двигуна з балансованим і небалансованим ротором є змішаними. Виявлено полігармонійність спектрів детермінованих коливань та визначено амплітуди гармонік.

Висновки. Запропоновані індикатори вібраційного стану двигунів можуть бути використані для їх балансування у процесі налагодження та ремонту. Подальші дослідження будуть зосередженні на аналізі структури полігармонійності спектрів вібросигналів і розробці методології виявлення дефектів на ранніх стадіях розвитку.

Ключові слова: газотурбінний двигун, вібрація, періодичні нестаціонарні випадкові процеси, частотна оцінка, середнє, дисперсія.